Ann Med Res

Current issue list available at AnnMedRes

Annals of Medical Research

journal page: www.annalsmedres.org

Evaluation of white matter properties in sinus vein thrombosis with diffusion tensor imaging

Serdar Balsak[a], Aslı Yaman Kula[b,*]

[a] *Bezmialem University, Faculty of Medicine, Department of Radiology, Istanbul, Türkiye*
[b] *Bezmialem University, Faculty of Medicine, Department of Neurology, Istanbul, Türkiye*

ARTICLE INFO

Keywords:
Diffusion tensor imaging
White matter
Sinus vein thrombosis

Received: Sep 05, 2024
Accepted: Oct 23, 2024
Available Online: 25.10.2024

DOI:
10.5455/annalsmedres.2024.09.185

Abstract

Aim: Brain MRI findings in sinus vein thrombosis (SVT) have been well described in many studies. However, to our knowledge, there is no diffusion tensor imaging (DTI) study in these cases in the literature. The main purpose of this article is to examine white matter integrity in SVT and to better understand the possible underlying white matter damage.

Materials and Methods: Our retrospective study is a neuroimaging study including 1.5 T MRI and brain DTI to evaluate the white matter integrity of patients with SVT and healthy controls. White matter DTI abnormalities were evaluated according to ROI. DTI findings of cases and healthy controls were compared.

Results: In cases with SVT, higher apparent diffusion coefficiency (ADC) values were detected in middle cerebellar peduncle, optic radiatio compared to healthy controls. Decreased fractional anisotrophy (FA) values were detected in cingulum, corona radiata, corpus callosum splenium, anterior limb of internal capsule, posterior limb of internal capsule, optic radiatio and corticospinal tract. High radial diffusivity (RD) values were detected in cingulum, corona radiata, superior longitudinal fasciculus, anterior limb of internal capsule, posterior limb of internal capsule, middle cerebellar peduncle, optic radiatio and corticospinal tract. Low axial diffusivity (AD) values were detected in cingulum, posterior limb of internal capsule and corticospinal tract.

Conclusion: Our findings may suggest intercellular edema and axon and myelin damage in white matter tracts in sinus thrombosis. DTI findings may be useful in quantitatively monitoring the response to treatment.

Introduction

Sinus vein thrombosis (SVT) is a cerebrovascular disease that mostly affects young women. The most common symptom in acute SVT is headache. Complications associated with SVT such as cerebral hemorrhage, intracranial hypertension, recurrent SVT or dural arteriovenous fistula (dAVF) may cause multiple emergency department visits. Since primary headache disorders, namely migraine and tension-type headaches, are also very common in the same age group, diagnosis may be delayed [1]. Variable symptoms of SVT make diagnosis difficult. The clinical picture is divided into 3 subgroups according to the onset time: acute, subacute and chronic. It can be encountered in clinical practice in acute-subacute and chronic forms, most commonly in subacute presentation. Recent advancements in magnetic resonance imaging (MRI) technology have led to a ten-fold increase in the prevalence of SVT and a global increase in its recognition. Its greater prevalence in females is most likely caused by oral contraceptive use, puberty, and pregnancy. Clinical symptoms such intracranial hypertension, focal neurological syndrome, diffuse encephalopathy, and cavernous sinus syndrome can all be present in patients with SVT. Slowly developing pathophysiological alterations in SVT might take weeks to manifest, resulting in SVT symptoms and indications. Intracranial blood volume rises as a result of elevated venous pressure brought on by cerebral vein thrombosis. Patients experience intracranial hypertension as a result. Vasogenic edema develops as a result of intracranial hypertension, which also causes the blood-brain barrier to become disrupted [2].

In T2-weighted sequences, the flow in normal open dural sinuses is defined as flow void. This flow void concept appears as signalless hypointense in T2-weighted sequences. In sinus thrombosis, loss is observed in this flow void due to flow loss and signal increase develops in the dural si-

*Corresponding author:
Email address: dr.asliyaman@gmail.com (Aslı Yaman Kula)

nus. Cerebral venous visibility is improved with contrast-enhanced MRV. When CT venography is unable to definitively diagnose a suspected case of deep vein thrombosis, magnetic resonance venography (MRV) can provide important information. On MR venography, however, transverse sinus hypoplasia can be mistaken for sinus thrombosis [3–6].

Diffusion tensor imaging (DTI) is an advanced imaging technique that can evaluate the microstructural integrity of the brain. The two most commonly used DTI parameters are FA and ADC. FA indicates the isotropy of the axon. Isotropy increases in cases of axonal damage. ADC is a parameter that can measure the extracellular distance sensitive to the diffusion of water molecules [7–10].

To date, white matter microstructural integrity has been evaluated in many diseases using the DTI method. Similarly, there are many MRI studies in the literature regarding SVT. However, to our knowledge, no DTI study has been reported in the literature regarding SVT. Our study investigates white matter integrity in acute SVT. Our study aims to reveal white matter microstructural changes in SVT.

Materials and Methods

Participants

For our retrospective study, patients who underwent brain MRI were identified by searching the keyword "sinus vein thrombosis" in our image archive system between April 2020-November 2021, with the approval (29.07.2024-159879) of our institution's ethics committee. Before starting our retrospective study, our institution's ethics committee approval was obtained. Based on the G*Power analysis, the minimum sample size required for the study was calculated to be 28 with a power of 87%, a type 1 error rate of 0.05, and an effect size of 0.3.

A total of 47 patients between the ages of 21-62 were evaluated for eligibility for the study. 30 patients with SVT (23 F, 7 M) diagnosed according to brain MRI and MRV findings were included in the study. 17 patients with intracranial tumors, hydrocephalus, atrophy, multiple sclerosis, and migraine comorbidities were excluded from the study (Figure 1). All patients underwent imaging during the symptomatic period. Therefore, all SVT patients were evaluated in the acute period. The control group of the study included 31 randomly selected controls (23 F, 8 M) from among patients who had no neurological disorder, no pathological findings in brain magnetic resonance imaging, and who underwent brain MRI for nonspecific reasons in accordance with the age and gender distribution of the patient group.

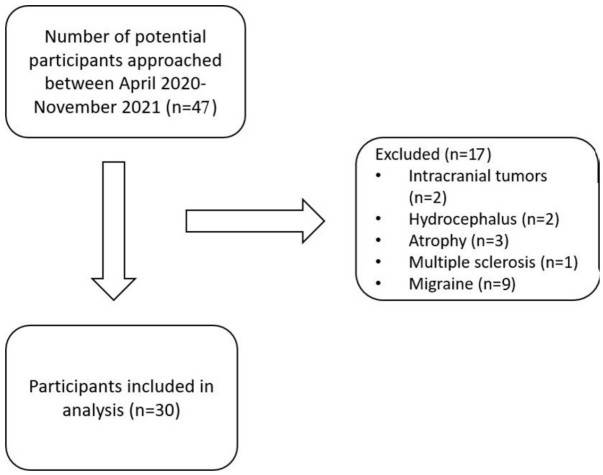

Figure 1. Flow diagram for the included and excluded patients with sinus vein thrombosis.

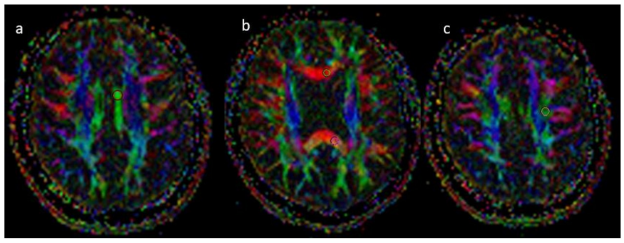

Figure 2. An examplifier case for ROI samplings from color-coded FA map images. Placement of the region of interests (ROIs) on the cingulum (A), corpus callosum genu and splenium (B), superior longitudinal fasciculus (C) on directionally color-coded map and anisotropy map.

MR imaging technique and DTI analysis

Before processing the images on the DTI workstation, a radiologist with 8 years of experience visually scanned all images. All MR images were obtained during the ictal period when the subjects complained of headache with 1.5 Tesla MRI (Avanto, Siemens Healthineers, Erlangen, Germany). Axial T1-weighted imaging (TR/TE: 500/9 ms), axial T2-weighted imaging, and sagittal T2-weighted imaging comprised the MRI protocol (TR/TE:4750/87). With 5 mm slice thickness, 220 mm field of view (FOV), 30 gradient directions, TR = 4000 ms, TE = 77 ms, and b = 0 s/mm^2 and b = 1000 s/mm^2, DTI was produced using SE-EPI sequences. The matrix size was 128x128.

A approach based on regions of interest (ROI) was employed in DTI analysis. Using color-coded fractional anisotrophy (FA), Axial Diffusivity (AD), Radial Diffusivity (RD) maps and ADC, DTI values were computed using the Siemens Syngo-Via console (software version 2.0). ROIs were placed on predetermined anatomical regions on the FA color maps. There are ten different neuroanatomical regions including cingulum, corona raidata, superior longitudinal fasciculus (SLF), genu and splenium of corpus callosum (CCG and CCS), anterior limb of internal capsule (ALIC), posterior limb of internal capsule (PLIC), middle cerebellar peduncle (MCP), optic radiation (OR) and corticospinal tract (CST). All ROIs were manually drawn at the correct anatomical localization and had a circular shape with an area of approximately 20-30 mm^2. This multiple ROI analysis is also shown in Figure 2.

DTI parameters including ADC, FA, AD and RD values

were compared between healthy control group and SVT groups.

Statistical analysis

Descriptive statistics were provided as mean±standard deviation for data following a normal distribution and median (Interquartile range) for data not following a normal distribution. The distribution of the variables was looked at using the Shapiro-Wilks test. The Independent samples t-test or Mann-Whitney U test was conducted to compare groups according to their distrubation. IBM Corp. released SPSS in 2021. The analysis was conducted using IBM SPSS Statistics for Windows, Version 28.0 (Armonk, NY: IBM Corp). A type-I error rate of α=0.05 was used.

Results

Cingulum

RD values obtained from cingulum were significantly higher than healthy control (p<0.001). FA and AD values obtained from cingulum were significantly lower than healthy control (respectively, p<0.001, p=0.026).

Corona radiata

FA values obtained from corona radiata were significantly lower than healthy control (p<0.001).

RD values obtained from corona radiata were significantly higher than healthy control (p<0.001).

Corpus callosum splenium

FA values obtained from the corpus callosum splenium were significantly lower than those in the healthy control (p=0.022).

Anterior limb of internal capsule

FA values obtained from the anterior limb of internal capsule were significantly lower than those in the healthy control (p<0.001).

Posterior limb of internal capsule

FA and AD values obtained from the posterior limb of internal capsule were significantly lower than those of the healthy control (respectively, p<0.001, p=0.008).

RD values obtained from the posterior limb of internal capsule were significantly higher than those of the healthy control (p<0.001).

Middle cerebellar peduncle

ADC, RD and AD values obtained from middle cerebellar peduncle were significantly higher than healthy control (respectively, p<0.001, p<0.001, p<0.001).

Optic radiatio

ADC and RD values obtained from optic radiatio were significantly higher than healthy control (respectively, p=0.003, p<0.001).

FA values obtained from optic radiatio were significantly lower than healthy control (p<0.001).

Corticospinal tract

RD values obtained from corticospinal tract were significantly higher than healthy control (p=0.001).

FA and AD values obtained from corticospinal tract were significantly lower than healthy control (respectively, p<0.001, p=0.019).

DTI values for each group are presented in detail in Table 1.

Discussion

SVT is an important cause of treatable stroke in young patients, but is often underdiagnosed due to its nonspecific clinical presentation. Patent venous sinuses usually have low signal intensity on spin-echo images due to flow void due to venous flow. This flow void is best seen on T2-weighted and FLAIR images. Thrombosis on spin-echo images is seen as high signal in the affected sinuses as flow void loss due to flow disruption. During thrombus development, hemoglobin within the thrombus breaks down and its paramagnetic properties change over time. In hyperacute thrombus, it is slightly hyperintense on T2 and FLAIR images due to intracellular oxyhemoglobin, while in the acute stage, it may appear hypointense on T2 and FLAIR sequences due to the presence of intracellular deoxyhemoglobin. In the early and late subacute stages, thrombus appears hyperintense on T1-weighted images. Finally, chronic thrombus has a hypointense signal in all sequences due to hemosiderin [11–15]. In conventional MRI, local paramagnetic changes within the thrombus change the thrombus signal over time. Thrombus signal intensity has been used to estimate thrombus age [16]. DTI is an advanced neuroimaging technique that allows the assessment of white matter integrity and allows us to understand the microstructural properties of axonal pathways. Frequently used parameters with DTI are FA, ADC, RD and AD. High FA indicates an organized axon structure and physiologically the myelinated structure of the axon. Thus, decreased FA values are seen in conditions that cause axon and myelin damage and demyelination. Damage to the myelin sheath and a decrease in the number of axons are associated with increased extracellular fluid volume. AD is mainly related to axonal density. AD values decrease in axonal damage and degeneration. RD values may mainly represent myelination. RD values decrease in demyelination.

There are numerous DTI studies in the literature on acute arterial thrombosis. However, to our knowledge, there is no DTI study on acute SVT related to the venous system. Our study revealed significant microstructural changes indicating that white matter pathways are affected in acute SVT. Our study reveals that not only the white matter pathways adjacent to the thrombosed sinus vein but also other white matter pathways beyond the adjacent white matter are affected.

There are DTI studies in the literature on acute arterial ischemia. In acute ischemia, low ADC values and low FA values due to decreased intercellular space indicating acute damage in the cytotoxic edema area in the white matter have been reported. They reported that these findings may also be effective in predicting the prognosis of patients. In temporal follow-up, an increase in ADC values

Table 1. Detailed diffusion tensor imaging parameters for sinus vein thrombosis patients and healthy control group.

		Control Group n=31	SVT Patients n=30	p-value
CINGULUM_ADC	Mean ± SD / Median (IQR)	811.10 ± 73.71 / 803.00 (76.50)	832.60 ± 47.32 / 837.00 (59.50)	0.180[a]
CINGULUM_FA	Mean ± SD / Median (IQR)	551.90 ± 80.66 / 557.00 (65.50)	458.17 ± 79.49 / 455.00 (93.75)	0.000[a]
CINGULUM_RD	Mean ± SD / Median (IQR)	524.39 ± 77.55 / 526.00 (86.00)	594.83 ± 71.03 / 587.50 (83.00)	0.000[a]
CINGULUM_AD	Mean ± SD / Median (IQR)	1383.35 ± 156.53 / 1377.00 (175.00)	1307.33 ± 116.56 / 1291.00 (122.50)	0.026[b]
CR_ADC	Mean ± SD / Median (IQR)	728.42 ± 57.81 / 722.00 (60.00)	747.97 ± 61.76 / 736.50 (66.00)	0.143[b]
CR_FA	Mean ± SD / Median (IQR)	545.16 ± 58.77 / 544.00 (81.50)	476.20 ± 72.76 / 482.50 (65.75)	0.000[b]
CR_RD	Mean ± SD / Median (IQR)	484.03 ± 48.96 / 479.00 (50.50)	546.23 ± 78.48 / 525.00 (82.75)	0.000[b]
CR_AD	Mean ± SD / Median (IQR)	1198.19 ± 89.03 / 1171.00 (132.00)	1153.37 ± 87.73 / 1140.00 (124.00)	0.052[a]
SLF_ADC	Mean ± SD / Median (IQR)	751.87 ± 44.24 / 753.00 (48.50)	763.67 ± 47.22 / 759.50 (56.50)	0.319[a]
SLF_FA	Mean ± SD / Median (IQR)	468.94 ± 58.60 / 471.00 (81.50)	448.07 ± 47.88 / 429.50 (69.50)	0.133[a]
SLF_RD	Mean ± SD / Median (IQR)	553.29 ± 54.63 / 551.00 (62.00)	576.73 ± 50.82 / 574.00 (61.25)	0.088[a]
SLF_AD	Mean ± SD / Median (IQR)	1150.94 ± 85.49 / 1138.00 (117.00)	1155.90 ± 76.21 / 1145.50 (75.25)	0.811[a]
CCGENU_ADC	Mean ± SD / Median (IQR)	883.16 ± 79.28 / 880.00 (84.50)	904.43 ± 158.91 / 867.00 (114.50)	0.740[b]
CCGENU_FA	Mean ± SD / Median (IQR)	698.97 ± 54.08 / 708.00 (71.50)	694.70 ± 84.25 / 715.00 (127.00)	0.816[a]
CCGENU_RD	Mean ± SD / Median (IQR)	450.39 ± 77.96 / 445.00 (88.50)	472.07 ± 179.63 / 429.00 (156.25)	0.676[b]
CCGENU_AD	Mean ± SD / Median (IQR)	1748.81 ± 153.49 / 1765.00 (190.50)	1768.47 ± 162.03 / 1746.00 (144.00)	0.983[b]
CCSPLENİUM_ADC	Mean ± SD / Median (IQR)	913.32 ± 105.11 / 908.00 (160.50)	921.50 ± 102.75 / 900.00 (151.50)	0.760[a]
CCSPLENİUM_FA	Mean ± SD / Median (IQR)	757.58 ± 50.23 / 752.00 (56.00)	684.00 ± 144.83 / 688.00 (161.75)	0.022[b]
CCSPLENİUM_RD	Mean ± SD / Median (IQR)	426.39 ± 103.94 / 458.00 (175.50)	470.07 ± 137.51 / 433.50 (241.50)	0.168[a]
CCSPLENİUM_AD	Mean ± SD / Median (IQR)	1886.45 ± 171.73 / 1914.00 (213.50)	1824.30 ± 156.46 / 1828.50 (100.25)	0.064[b]
ALIC_ADC	Mean ± SD / Median (IQR)	763.90 ± 66.00 / 749.00 (64.00)	768.33 ± 81.18 / 762.50 (57.00)	0.367[b]
ALIC_FA	Mean ± SD / Median (IQR)	485.65 ± 53.44 / 478.00 (76.50)	428.00 ± 61.63 / 418.00 (91.25)	0.000[a]
ALIC_RD	Mean ± SD / Median (IQR)	534.52 ± 56.64 / 528.00 (53.50)	569.80 ± 82.12 / 568.00 (87.25)	0.057[a]
ALIC_AD	Mean ± SD / Median (IQR)	1222.94 ± 122.39 / 1186.00 (135.00)	1165.37 ± 118.65 / 1147.50 (106.25)	0.059[b]
PLIC_ADC	Mean ± SD / Median (IQR)	722.97 ± 30.94 / 723.00 (33.00)	738.30 ± 45.94 / 734.00 (46.25)	0.134[a]
PLIC_FA	Mean ± SD / Median (IQR)	666.61 ± 44.63 / 663.00 (62.50)	604.40 ± 57.44 / 603.00 (85.25)	0.000[a]
PLIC_RD	Mean ± SD / Median (IQR)	391.87 ± 38.97 / 391.00 (45.00)	446.00 ± 59.31 / 446.00 (62.25)	0.000[a]
PLIC_AD	Mean ± SD / Median (IQR)	1385.00 ± 87.39 / 1374.00 (122.50)	1322.70 ± 88.67 / 1325.50 (101.50)	0.008[a]
MCP_ADC	Mean ± SD / Median (IQR)	708.23 ± 31.27 / 704.00 (31.00)	818.63 ± 87.72 / 804.00 (107.00)	0.000[a]
MCP_FA	Mean ± SD / Median (IQR)	585.90 ± 54.11 / 584.00 (69.00)	599.77 ± 43.74 / 599.00 (62.75)	0.275[a]
MCP_RD	Mean ± SD / Median (IQR)	437.52 ± 44.39 / 445.00 (60.50)	507.70 ± 92.28 / 498.50 (94.00)	0.000[b]
MCP_AD	Mean ± SD / Median (IQR)	1249.55 ± 82.29 / 1243.00 (117.00)	1440.57 ± 110.25 / 1420.00 (158.50)	0.000[a]
OR_ADC	Mean ± SD / Median (IQR)	853.29 ± 75.56 / 852.00 (79.00)	940.67 ± 113.67 / 908.00 (180.00)	0.003[b]
OR_FA	Mean ± SD / Median (IQR)	553.16 ± 64.93 / 556.00 (91.50)	483.20 ± 55.62 / 487.50 (71.50)	0.000[a]
OR_RD	Mean ± SD / Median (IQR)	552.32 ± 85.71 / 554.00 (111.00)	669.97 ± 109.04 / 669.00 (153.75)	0.000[a]
OR_AD	Mean ± SD / Median (IQR)	1455.39 ± 122.54 / 1418.00 (134.50)	1481.67 ± 154.61 / 1452.00 (224.50)	0.609[b]
CST_ADC	Mean ± SD / Median (IQR)	742.87 ± 53.84 / 734.00 (43.50)	762.53 ± 64.59 / 764.00 (68.50)	0.097[b]
CST_FA	Mean ± SD / Median (IQR)	580.00 ± 72.63 / 571.00 (88.50)	500.63 ± 66.20 / 491.50 (58.25)	0.000[a]
CST_RD	Mean ± SD / Median (IQR)	478.74 ± 67.55 / 483.00 (66.50)	542.17 ± 75.27 / 553.00 (69.75)	0.001[a]
CST_AD	Mean ± SD / Median (IQR)	1271.42 ± 123.92 / 1243.00 (165.50)	1203.63 ± 97.98 / 1186.00 (103.75)	0.019[b]

[a]: Independent Sample-t test, [b]: Mann-Whitney U Test n, number of subjects; ADC, apparent diffusion coefficient; FA, fractional anisotropy; RD, radial diffusivity; AD, axial diffusivity. Data were presented with mean ± standard deviation and Median (IQR).

has been reported as a result of increased intercellular fluid as cytotoxic edema gives way to vasogenic edema [17, 18]. Vasogenic edema may develop due to congestion in the white matter in SVT [19]. In a DTI study conducted on the vasogenic edema area developing in the white matter due to venous ischemia, they reported microstructural changes indicating increased fluid accumulation between axons and developing axonal degeneration [20]. In our study, we found high ADC values representing vasogenic edema and low FA values representing axonal degeneration and damage developing as a result of this in many white matter pathways in the acute period after sinus thrombosis. We also found high RD and low AD values indicating impaired axonal density and myelin damage. DTI is an advanced neuroimaging method that detects white matter microstructural changes before macroscopic changes [21]. In parallel with this, we found high ADC values in the white matter even in cases where vasogenic edema was not observed in the white matter. This shows the high sensitivity of the DTI technique to microstructural changes in the white matter that occur before morphological findings and are not yet detected by conventional MRI.

Limitations

Our study has some limitations other than being a retrospective single-center study. ROI-based approach may

show operator-dependent variability. Therefore, we think that channel-based spatial statistics (TBSS) will be more important for future studies. We think that in order to understand the effect of SVT on white matter, long-term cohort studies with a larger patient group will be necessary in the future to determine how white matter microstructural changes are affected in the subacute and long-term follow-up, apart from the acute period.

Conclusion

SVT is an important cause of headache that can be treated. Although brain MRI findings in SVT are well-defined, white matter microstructural changes are not found in the literature. Our study emphasizes DTI parameters suggesting that microstructural integrity is lost not only in the white matter adjacent to the thrombosed sinus, but also in many pathways of the white matter. We thought that the potential mechanism underlying this microstructural damage could be edema and axonal damage due to pressure changes that occur after venous congestion. DTI changes may be useful in monitoring these cases and in quantitatively assessing response to treatment. Future follow-up DTI studies outside the acute phase are needed to determine whether microstructural findings of SVT can be reversed after treatment.

Ethical approval

Bezmialem Vakif University ethics committee approved the study (29.07.2024-159879).

References

1. Dias L, João Pinto M, Maia R, Albuquerque L, Carvalho M. Post cerebral venous thrombosis headache - Prevalence, mechanisms and risk factors. J Clin Neurosci. 2024 Jan;119:205-211. doi: 10.1016/j.jocn.2023.12.005. Epub 2023 Dec 22. PMID: 38141436.
2. Ranjan R, Ken-Dror G, Sharma P. Pathophysiology, diagnosis and management of cerebral venous thrombosis: A comprehensive review. Medicine (Baltimore). 2023 Dec 1;102(48):e36366. doi: 10.1097/MD.0000000000036366. PMID: 38050259; PMCID: PMC10695550.
3. Wasay M, Bakshi R, Bobustuc G, et al. Cerebral venous thrombosis: analysis of a multicenter cohort from the United States. J Stroke Cerebrovasc Dis. 2008;17:49–54.
4. Einhäupl K, Stam J, Bousser MG, et al. EFNS guideline on the treatment of cerebral venous and sinus thrombosis in adult patients. Eur J Neurol. 2010;17:1229–35.
5. Qu H, Yang M. Early imaging characteristics of 62 cases of cerebral venous sinus thrombosis. Exp Ther Med. 2013;5:233–6.
6. Leach JL, Fortuna RB, Jones BV, et al. Imaging of cerebral venous thrombosis: current techniques, spectrum of findings, and diagnostic pitfalls. Radiographics. 2006;26:S19–41; discussion S42.
7. Yuzkan S, Hasimoglu O, Balsak S, Mutlu S, Karagulle M, Kose F, Altinkaya A, Tugcu B, Kocak B. Utility of diffusion tensor imaging and generalized q-sampling imaging for predicting short-term clinical effect of deep brain stimulation in Parkinson's disease. Acta Neurochir (Wien). 2024 May 15;166(1):217. doi: 10.1007/s00701-024-06096-w. PMID: 38748304; PMCID: PMC11096246.
8. Balsak S, Atasoy B, Donmez Z, Yabul FC, Daşkaya H, Akkoyunlu Y, Yurtsever İ, Sarı L, Sijahovic S, Akcay A, Toluk O, Alkan A. Microstructural alterations in hypoxia-related BRAIN centers after COVID-19 by using DTI: A preliminary study. J Clin Ultrasound. 2023 Sep;51(7):1276-1283. doi: 10.1002/jcu.23503. Epub 2023 Jun 9. PMID: 37293861.
9. Yurtsever I, Atasoy B, Bozkurt S, Yıldız GB, Balsak S, Yabul F, Donmez Z, Selvitop R, Karaman O, Toluk O, Alkan A. Diffusion tensor imaging findings in the hunger and satiety centers of the brain after bariatric surgery: a preliminary study. Ir J Med Sci. 2024 Feb;193(1):191-197. doi: 10.1007/s11845-023-03389-4. Epub 2023 May 25. PMID: 37231150.
10. Atasoy B, Balsak S, Donmez Z, Yurtsever I, Yabul F, Akcay A, Atila N, Cesme DH, Toluk O, Alkan A. Evaluation of the white matter integrity in morbidly obese patients before and after bariatric surgery; a diffusion tensor imaging study. J Clin Ultrasound. 2023 Oct;51(8):1403-1409. doi: 10.1002/jcu.23550. Epub 2023 Aug 29. PMID: 37644657.
11. Hedlund GL (2013) Cerebral sinovenous thrombosis in pediatric practice. Pediatr Radiol 43:173–188.
12. Isensee C, Reul J, Thron A (1994) Magnetic resonance imaging of thrombosed dural sinuses. Stroke 25:29–34.
13. Lafitte F, Boukobza M, Guichard JP, Hoeffel C, Reizine D, Ille O, Woimant F, Merland JJ (1997) MRI and MRA for diagnosis and follow-up of cerebral venous thrombosis (CVT). Clin Radiol 52:672–679.
14. Dormont D, Anxionnat R, Evrard S, Louaille C, Chiras J, Marsault C (1994) MRI in cerebral venous thrombosis. J Neuroradiol 21:81–99.
15. Bianchi D, Maeder P, Bogousslavsky J, Schnyder P, Meuli RA (1998) Diagnosis of cerebral venous thrombosis with routine magnetic resonance: an update. Eur Neurol 40:179–190.
16. Wagner MW, Bosemani T, Oshmyansky A, Poretti A, Huisman TA. Neuroimaging findings in pediatric cerebral sinovenous thrombosis. Childs Nerv Syst. 2015 May;31(5):705-12. doi: 10.1007/s00381-015-2662-1. Epub 2015 Feb 26. PMID: 25715842.
17. Keijzer HM, Duering M, Pasternak O, Meijer FJA, Verhulst MMLH, Tonino BAR, Blans MJ, Hoedemaekers CWE, Klijn CJM, Hofmeijer J. Free water corrected diffusion tensor imaging discriminates between good and poor outcomes of comatose patients after cardiac arrest. Eur Radiol. 2023 Mar;33(3):2139-2148. doi: 10.1007/s00330-022-09245-w. Epub 2022 Nov 24. PMID: 36418623; PMCID: PMC9935650.
18. Osa García A, Brambati SM, Desautels A, Marcotte K. Timing stroke: A review on stroke pathophysiology and its influence over time on diffusion measures. J Neurol Sci. 2022 Oct 15;441:120377. doi: 10.1016/j.jns.2022.120377. Epub 2022 Aug 2. PMID: 36049374.
19. Saposnik G, Bushnell C, Coutinho JM, Field TS, Furie KL, Galadanci N, Kam W, Kirkham FC, McNair ND, Singhal AB, Thijs V, Yang VXD; American Heart Association Stroke Council; Council on Cardiopulmonary, Critical Care, Perioperative and Resuscitation; Council on Cardiovascular and Stroke Nursing; and Council on Hypertension. Diagnosis and Management of Cerebral Venous Thrombosis: A Scientific Statement From the American Heart Association. Stroke. 2024 Mar;55(3):e77-e90. doi: 10.1161/STR.0000000000000456. Epub 2024 Jan 29. PMID: 38284265.
20. Yu X, Yin X, Hong H, Wang S, Jiaerken Y, Xu D, Zhang F, Zhang R, Yang L, Zhang B, Zhang M, Huang P. Presumed periventricular venous infarction on magnetic resonance imaging and its association with increased white matter edema in CADASIL. Eur Radiol. 2023 Nov;33(11):8057-8066. doi: 10.1007/s00330-023-09744-4. Epub 2023 Jun 7. PMID: 37284868.
21. Tedeschi G, Russo A, Conte F, et al. Increased interictal visual network connectivity in patients with migraine with aura. Cephalalgia. 2016;36(2):139-147. doi:10.1177/0333102415584360.